Herschel: the first science highlights

Letter to the Editor

Detection of interstellar oxidaniumyl: Abundant H₂O⁺ towards the star-forming regions DR21, Sgr B2, and NGC6334[⋆]

V. Ossenkopf[1,2], H. S. P. Müller[1], D. C. Lis[3], P. Schilke[1,4], T. A. Bell[3], S. Bruderer[8], E. Bergin[5], C. Ceccarelli[6], C. Comito[4], J. Stutzki[1], A. Bacman[6,7], A. Baudry[7], A. O. Benz[8], M. Benedettini[9], O. Berne[36], G. Blake[3], A. Boogert[3], S. Bottinelli[13], F. Boulanger[10], S. Cabrit[11], P. Caselli[12], E. Caux[13,14], J. Cernicharo[15], C. Codella[16], A. Coutens[13], N. Crimier[6,15], N. R. Crockett[5], F. Daniel[11,15], K. Demyk[13], P. Dieleman[2], C. Dominik[18,19], M. L. Dubernet[20], M. Emprechtinger[3], P. Encrenaz[11], E. Falgarone[17], K. France[27], A. Fuente[21], M. Gerin[17], T. F. Giesen[1], A. M. di Giorgio[9], J. R. Goicoechea[15], P. F. Goldsmith[22], R. Güsten[4], A. Harris[23], F. Helmich[2], E. Herbst[24], P. Hily-Blant[6], K. Jacobs[1], T. Jacq[7], Ch. Joblin[13,14], D. Johnstone[25], C. Kahane[6], M. Kama[18], T. Klein[4], A. Klotz[13], C. Kramer[26], W. Langer[22], B. Lefloch[6], C. Leinz[4], A. Lorenzani[16], S. D. Lord[3], S. Maret[6], P. G. Martin[27], J. Martin-Pintado[15], C. McᶜCoey[28,41], M. Melchior[29], G. J. Melnick[30], K. M. Menten[4], B. Mookerjea[40], P. Morris[3], J. A. Murphy[31], D. A. Neufeld[32], B. Nisini[33], S. Pacheco[6], L. Pagani[10], B. Parise[4], J. C. Pearson[22], M. Pérault[11], T. G. Phillips[3], R. Plume[34], S.-L. Quin[1], R. Rizzo[21], M. Röllig[1], M. Salez[11], P. Saraceno[9], S. Schlemmer[1], R. Simon[1], K. Schuster[26], F. F. S. van der Tak[2,35], A. G. G. M. Tielens[36], D. Teyssier[37], N. Trappe[31], C. Vastel[13,14], S. Viti[38], V. Wakelam[7], A. Walters[13], S. Wang[5], N. Whyborn[39], M. van der Wiel[2,35], H. W. Yorke[22], S. Yu[22], and J. Zmuidzinas[3]

(Affiliations are available in the online edition)

ABSTRACT

Aims. We identify a prominent absorption feature at 1115 GHz, detected in first HIFI spectra towards high-mass star-forming regions, and interpret its astrophysical origin.
Methods. The characteristic hyperfine pattern of the H_2O^+ ground-state rotational transition, and the lack of other known low-energy transitions in this frequency range, identifies the feature as H_2O^+ absorption against the dust continuum background and allows us to derive the velocity profile of the absorbing gas. By comparing this velocity profile with velocity profiles of other tracers in the DR21 star-forming region, we constrain the frequency of the transition and the conditions for its formation.
Results. In DR21, the velocity distribution of H_2O^+ matches that of the [C II] line at 158 μm and of OH cm-wave absorption, both stemming from the hot and dense clump surfaces facing the H II-region and dynamically affected by the blister outflow. Diffuse foreground gas dominates the absorption towards Sgr B2. The integrated intensity of the absorption line allows us to derive lower limits to the H_2O^+ column density of 7.2×10^{12} cm^{-2} in NGC 6334, 2.3×10^{13} cm^{-2} in DR21, and 1.1×10^{15} cm^{-2} in Sgr B2.

Key words. astrochemistry – line: identification – molecular data – ISM: abundances – ISM: molecules – ISM: clouds

1. Introduction

Oxidaniumyl or oxoniumyl (Connelly et al. 2005), the reactive water cation, H_2O^+, plays a crucial role in the chemical network describing the formation of oxygen-bearing molecules in UV irradiated parts of molecular clouds (van Dishoeck & Black 1986; Gerin et al. 2010). It was identified at optical wavelengths in the tails of comets in the 1970's (Fehrenbach & Arpigny 1973; Herzberg & Lew 1974; Wehinger et al. 1974), but its detection in the general interstellar medium has proven elusive.

We report a detection of the ground-state rotational transition of H_2O^+ in some of the first spectra taken with the HIFI instrument (de Graauw et al. 2010) on board the *Herschel* Space Observatory (Pilbratt et al. 2010) during the performance verification campaign and early science observations. Section 2 briefly introduces the properties of the sources where H_2O^+ was

detected. Section 3 summarises the spectroscopic data of the molecule. The observations and the line identification are described in Sects. 4 and 5 we discuss the physical properties of the H_2O^+ absorption layer.

2. The sources

We observed three massive Galactic star-forming/H II regions with very different properties. The DR21 star-forming region is embedded in a ridge of dense molecular material that obscures it at optical wavelengths. The embedded cluster drives a violent bipolar outflow and creates bright photon-dominated (or photodissociation) regions (PDRs), visible as clumps of 8 μm PAH emission in *Spitzer* IRAC maps (Marston et al. 2004) and showing up in emission lines from tracers of irradiated hot gas, such as HCO⁺, high-J CO, atomic and ionised carbon, and atomic oxygen (Lane et al. 1990; Jakob et al. 2007). The eastern, blueshifted outflow expands in a blister-like fountain, while the western, red-shifted outflow is confined to a small cone.

Table 1. Parameters of the hyperfine lines $F' - F''$ in the observed $1_{11}-0_{00}$, $J = 3/2-1/2$ ortho H$_2$O$^+$ transition, including predicted frequencies, Einstein-A and optical depth at low temperatures.

$F' - F''$	$\nu_{\text{Mürtz}}^a$ [MHz]	ν_{Strahan}^a [MHz]	$\nu_{\text{OH-based}}^b$ [MHz]	A [s^{-1}]	$\int \tau dv$ _c_
5/2–3/2	1 115 204.1	1 115 175.8	1 115 161	0.031	23.51
3/2–1/2	1 115 150.5	1 115 122.0	1 115 107	0.017	8.67
3/2–3/2	1 115 263.2	1 115 235.6	1 115 221	0.014	7.00
1/2–1/2	1 115 186.2	1 115 158.0	1 115 143	0.027	6.96
1/2–3/2	1 115 298.9	1 115 271.6	1 115 257	0.0035	0.88

Notes. [a] Predictions based on Strahan et al. (1986) and Mürtz et al. (1998). Nominal uncertainties are $\approx$ 2 MHz but this is inconsistent with the discrepancy between the two predictions so that the actual uncertainty is unknown; [b] from the matching DR21 OH pattern by Guilloteau et al. (1984); [c] $\int \tau_{\text{low-}T}/N_{\text{H}_2\text{O}^+}dv$ in 10^{-14} km s^{-1} cm^2.

Table 2. Summary of the observational parameters.

	DR21(C)	Sgr B2(M)	NGC 6334
RA (J2000)	20h39m01.1s	17h47m20.35s	17h20m53.32s
Dec	42°19′43.0″	−28°23′03.0″	−35°46′58.5″
Mode	Load-chop[2]	DBS	DBS
$t_{\text{int,source}}$	150 s	48 s	48 s
σ_{noise}^1	0.07 K	0.08 K	0.08 K

Notes. [1] At native WBS resolution (1.1 MHz = 0.30 km s^{-1}).
[2] OFF position = 20h37m10s, 42°37′00″.

The Sgr B2(M) and (N) cores are the most massive star-formation sites in our Galaxy. The line of sight, located in the plane of the Galaxy, passes through many spiral arm clouds and the extended envelope of Sgr B2 itself. The foreground clouds display a very rich molecular and atomic spectrum (Polehampton et al. 2007), although they often have very low densities and column densities, characteristic of diffuse or translucent clouds. The envelope of Sgr B2 itself includes hot, low density layers at both the ambient cloud velocity of 64 km s^{-1}, and at 0 km s^{-1} (Ceccarelli et al. 2002). Many species detected along this line of sight have not been found elsewhere and the exact origin of the molecular features is often ambiguous because of the overlapping radial velocities (e.g., Comito et al. 2003).

NGC 6334 is a nearby molecular cloud complex containing several concentrations of massive stars at various stages of evolution. The far-infrared source "I" contains an embedded cluster of NIR sources (Tapia et al. 1996). Four compact mm continuum sources are located near the geometric centre of the cluster (Hunter et al. 2007). Although NGC 6334I is not known to exhibit strong absorption lines, its OH absorption profiles (Brooks & Whiteoak 2001) reveal two molecular clouds along this line of sight, one with velocities between −15 and 2 km s^{-1}, and the other near 6 km s^{-1}.

3. The H$_2$O$^+$ spectroscopy

The H$_2$O$^+$ cation is a radical with a $^2B_1$ electronic ground state and bond lengths and angle slightly larger than H$_2$O. Quantum-chemical calculations (Weis et al. 1989) yield a ground-state dipole moment of 2.4 D. The B_1 symmetry of the ground electronic state leads to a reversal of the *ortho* and *para* levels relative to water.

The rotational spectrum was measured by laser magnetic resonance (Strahan et al. 1986; Mürtz et al. 1998). Predictions of the
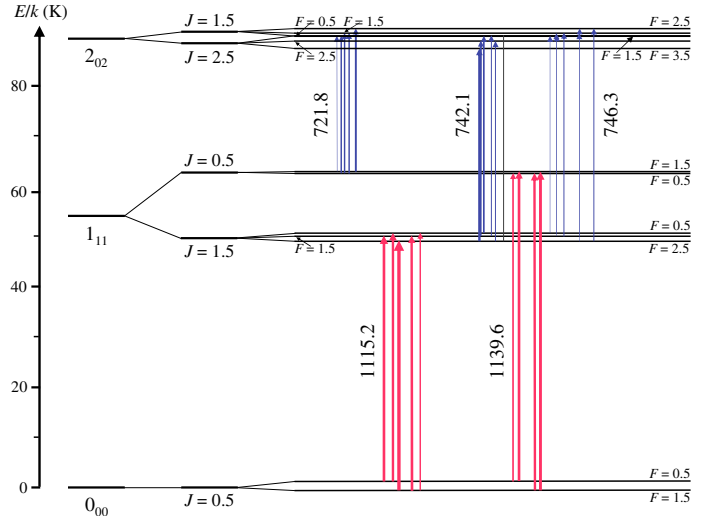
Fig. 1. Energy level diagram of the lowest rotational levels of *ortho*-H$_2$O$^+$ and its radiative transitions. The fine structure transition frequencies are given in GHz.

$N_{K_aK_c} = 1_{11}-0_{00}$, $J = 3/2-1/2$ fine structure component near 1115 GHz using the new parameters by Mürtz et al. (1998) are between 27.3 and 28.5 MHz higher than those calculated from Strahan et al. (1986), even though both articles claim to have reproduced the experimental data to $\sim$2 MHz. The reanalysis of equivalent measurements of SH$^+$, by Brown & Müller (2009), shows that this accuracy is in principle achievable. However, the large centrifugal distortion in H$_2$O$^+$ requires a large set of spectroscopic parameters to reproduce a comparatively small set of data; this may cause problems in the zero-field extrapolation. Moreover, the frequencies of the two fine structure levels of the 1_{11} rotational state in Table V of Mürtz et al. (1998) agree precisely with those of the $F' = J'$, $F'' = J''$ hyperfine transitions. This can only be achieved when the calculated frequencies are lower by 51.56 and 88.05 MHz, respectively, since the respective hyperfine component is the lowest in each case. Correcting the published frequencies of the $J = 3/2-1/2$ fine structure component by 51.56 MHz improves the agreement with Strahan et al. (1986). The results are summarized in Table 1. Alternatively, we could use the corrected frequencies of Mürtz et al. (1998) and arrive at values that are lower by about 23 MHz. This provides a rough estimate of the uncertainty in the predictions. An H$_2$O$^+$ catalogue entry will be prepared for the CDMS (Müller et al. 2005) by carefully scrutinizing the available IR data summarised in Zheng et al. (2008, and references therein) with $\approx$150 MHz uncertainties.

4. Observations of the 1115 GHz ground-state transition

The H$_2$O$^+$ line was detected in DR21 during performance verification observations of the HIFI instrument, testing spectral scans in the HIFI band 4b. Later science observations of Sgr B2 and NGC 6334 also confirmed the detection in these sources using the identification and frequency assignment from DR21. The main parameters of the observations are summarised in Table 2. At 1115 GHz, the *Herschel* beam has 21″ HPBW.

The identification with H$_2$O$^+$ was straightforward in DR21 because of the simple source velocity structure that cannot be confused with the well resolved, characteristic hyperfine structure of the line. When fitting the line, one has to take into account that the line extinction begins to saturate, with a maximum optical depth of 0.59 for DR21 and 1.55 for Sgr B2 (see below). For
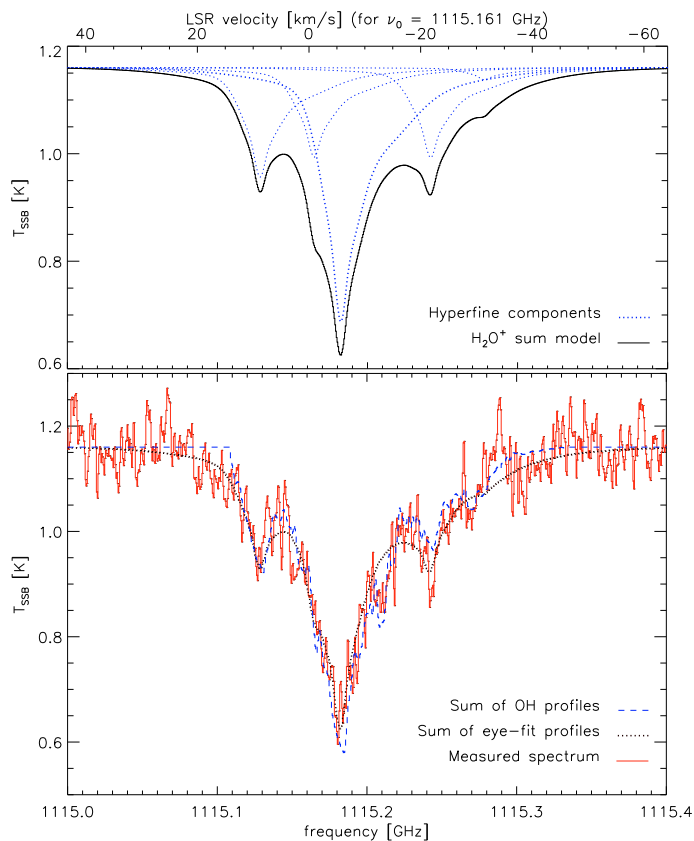
Fig. 2. Fit of the hyperfine multiplet of the H_2O^+1115 GHz line in DR21. The bottom panel shows the 0.5 K absorption line superimposed on two different fit profiles, one based on a 3-component Gaussian (see text) and the other one using the OH 6 cm absorption spectrum from Guilloteau et al. (1984). The top panel shows a breakdown of the fitted profile into its hyperfine constituents in the case of the 3-Gaussian profile.

DR21, we fitted the observed profile using an adjusted velocity profile with asymmetric wings. Because of the limited signal-to-noise ratio, the fit was performed manually by adding three Gaussian components of increasing width (see Fig. 2).

The resulting velocity distribution allows us to interpret the origin of the absorbing material by comparing with the velocity distribution of other species observed towards the same position with comparable beam size (see Ossenkopf et al. 2010; Falgarone et al. 2010; van der Tak et al. 2010). Figure 3 shows that the peak H_2O^+ velocity of -1.7 km s^{-1} is not seen in any other tracer. The intrinsic velocity of the DR21 molecular ridge is -3.0 km s^{-1}, which is matched by the line centres of the $H^{13}CO^+$ 1–0, the CO 6–5, and the ^{13}CO 6–5 transitions. The higher excitation lines of ^{13}CO, $C^{18}O$, H_2O, and the [C II] line exhibit a slightly blue-shifted peak velocity of about -5.0 km s^{-1}. The H_2O^+ profile exhibits a prominent, very broad blue wing. This is not present in any of the molecular emission lines, but is found in the [C II] profile and the OH absorption spectrum measured by Guilloteau et al. (1984) towards the same position.

To underline this good match, we have superimposed in Fig. 2 the absorption profile that would be obtained by simply performing the hyperfine superposition of the 6.030 GHz OH absorption profile. The match is as good as that achieved with the analytic profile and even reproduces the small excursions at 1115.22 and 1115.27 GHz. This indicates that OH and H_2O^+ occur in the same region and under the same physical conditions. The displacement of the fitted profile relative to the [C II]
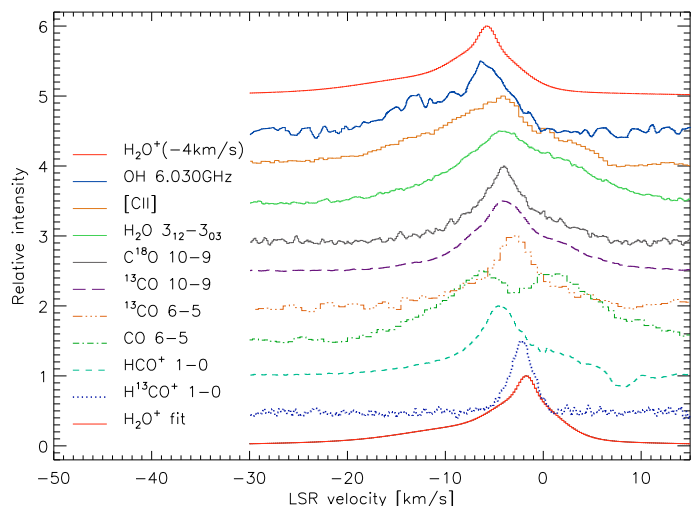
Fig. 3. Comparison of the fitted H_2O^+velocity profile to other tracers observed in DR21 with similar beam size. The profiles are normalised to a peak of unity and separated by multiples of 0.5 *from bottom to top*. The fit (*bottom line*) used the Strahan et al. (1986) based line frequency prediction, the profile at the top is shifted by -4.0 km s^{-1}, corresponding to a rest frequency lower by 15 MHz.

and OH profiles of about 4.0 km s^{-1} is within the discrepancies between the different predictions of the line frequency. The astronomically determined line rest frequencies from comparison with the OH line fall 15 MHz below the predicted frequencies. As the line peak is very sharp, the accuracy of the frequency is probably better than 2 MHz. Assuming a match with the [C II] line instead, would provide a larger uncertainty of the order of 6 MHz.

The identification and the corrected frequencies are then used to analyse the line structures in Sgr B2 and NGC 6334 (Figs. 4 and 5). In Sgr B2, we see absorption at both the velocity of its envelope and the velocities of many foreground clouds, almost saturating the line. NGC 6334 exhibits weak H_2O^+ absorption at -13 km s^{-1}. This deviates from the OH absorption profile towards the source measured by Brooks & Whiteoak (2001). At velocities below -10 km s^{-1}, only some OH maser emission was found. This might indicate that the observed H_2O^+ is not related to the foreground material, but to hot gas in the direct vicinity of the continuum sources. Alternatively, if we use the predicted frequencies from Strahan et al. (1986) in Table 1, the H_2O^+ absorption in NGC 6334 is centred on -9 km s^{-1}, in reasonable agreement with the OH absorption at -8.2 km s^{-1} measured toward component F[1]. At about -9 km s^{-1}, Beuther et al. (2005) also observed CH_3OH and NH_3 absorption towards the H II region.

5. Discussion and outlook

That H_2O^+ shows up in absorption against the dust continuum implies that the excitation of the molecule must be colder than the dust. As a reactive ion (see the discussion by Black 2007; Stäuber & Bruderer 2009, for CO$^+$), H_2O^+ is not expected to be in thermal equilibrium at the kinetic temperature of the gas. Its excitation reflects either the chemical formation process or the

---

[1] A similar case is reported by Gerin et al. (2010) for W31C. The source shows a complicated spectrum with multiple absorption components, but a closer correlation with other tracers is found when using the Strahan et al. (1986) based frequencies. A recent detection of H_2O^+in W3 IRS5 and AFGL2591 by Benz et al. (in prep.) seems to favour the frequency predictions by Mürtz et al. (1998).
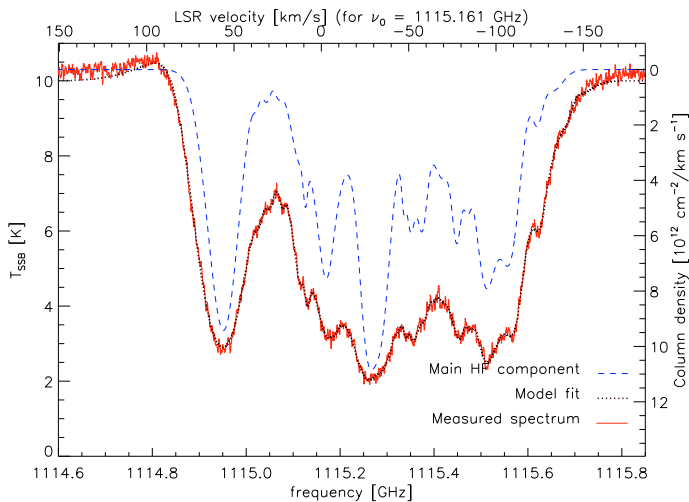
Fig. 4. Fit of the observed H_2O^+ line in Sgr B2. The dashed line visualises the velocity structure of the absorbers by plotting the strongest hyperfine component on a linear column density scale, i.e., without optical depth correction.
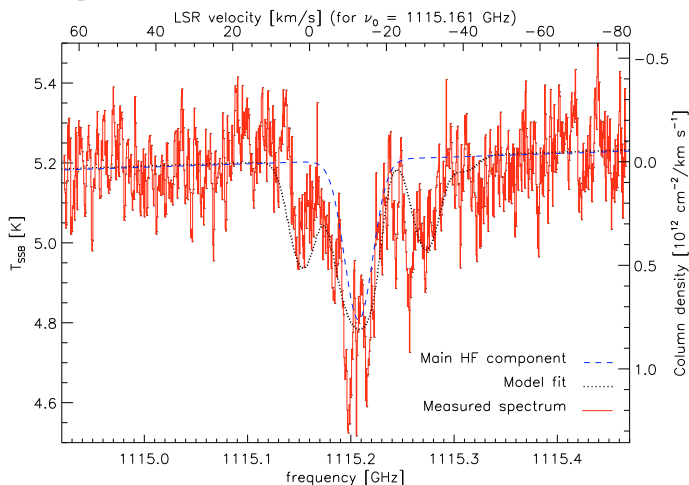
Fig. 5. Same as Fig. 4, but for NGC 6334.

radiative coupling with the environment. From a single absorption line, one can only provide a lower limit to the H_2O^+ column density, assuming a low excitation temperature where basically all H_2O^+ resides in the ground state, which is applicable to temperatures well below the upper level energy of 53 K.

Table 1 provides the integral over the optical depth of the hyperfine components in the low temperature limit. For the overall $J = 3/2-1/2$ fine structure transition, we obtain a line integrated optical depth of $\int \tau d\nu / N_{H_2O^+} = 4.70 \times 10^{-13}$ km s^{-1} cm^2 per molecule, resulting in a lower limit to the H_2O^+ ground-state column densities of 7.2×10^{12} cm^{-2} for NGC 6334, 2.3×10^{13} cm^{-2} for DR21, and 1.1×10^{15} cm^{-2} for Sgr B2.

These values are lower limits not only because of to the low-temperature approximation, but also because they assume that the absorption occurs in front of the continuum source and not within the dusty cloud, where the line absorption is partially compensated by dust emission. There may also be additional amounts of H_2O^+ in the para species that would not contribute to the 1115 GHz line. Altogether, the total H_2O^+ column density could be much higher than the lower limits given here.

The excellent correlation between the H_2O^+ profile and the OH absorption profile in DR21 indicates that both species occur in the same thin layer of hot gas (Jones et al. 1994) that directly faces the H II region at the blue-shifted blister outflow. There

is no obvious correlation with the distributions of CO, H_2O, or HCO$^+$. For Sgr B2, we can clearly identify absorption in multiple translucent foreground clouds. Their densities must be high enough to produce some molecular hydrogen, but low enough not to quickly destroy the H_2O^+. For NGC 6334, the gas component producing the H_2O^+ absorption remains unidentified.

With the identification of H_2O^+ in the interstellar medium, we provide a first step to quantifying an important intermediate node in the oxygen chemical network, connecting OH$^+$ in diffuse clouds and at cloud boundaries, through H_3O^+, with water in denser and cooler cloud parts. To obtain an estimate for the total H_2O^+ abundance, we need to measure the excitation temperature of H_2O^+. Observations of additional transitions of H_2O^+, such as those at 742 GHz, are therefore essential.

References

Beuther, H., Thorwirth, S., Zhang, Q., et al. 2005, ApJ, 627, 834
Black 2007, in Molecules in Space and Laboratory, ed. J. L. Lemaire, & F. Combes, (S. Diana publ.), 90
Brooks, K. J., & Whiteoak, J. B. 2001, MNRAS, 320, 465
Brown, J. M., & Müller, H. S. P. 2009, J. Mol. Spectrosc., 255, 68
Ceccarelli, C., Baluteau, J., Walmsley, M., et al. 2002, A&A, 383, 603
Comito, C., Schilke, P., Gerin, M., et al. 2003, A&A, 402, 635
Connelly, N. G., Hartshorn, R. M., Damhus, T., & Hutton, A. T. 2005, Nomenclature of Inorganic Chemistry, International Union of Pure and Applied Chemistry (RSC Publishing), 110
de Graauw, Th., Helmich, F. P., Phillips, T. G., et al. 2010, A&A, 518, L6
Falgarone, E., Ossenkopf, V., Gerin, M., et al. 2010, A&A, 518, L118
Fehrenbach, C., & Arpigny, C. 1973, C. R. Acad. Sci. Paris, Sér. B, 277, 569
Gerin, M., de Luca, M., Black, J., et al. 2010, A&A, 518, L110
Guilloteau, S., Baudry, A., et al. 1984, A&A, 131, 45
Herzberg, G., & Lew, H. 1974, A&A, 31, 123
Jakob, H., Kramer, C., Simon, R., et al. 2007, A&A, 461, 999
Jones, K. N., Field, D., Gray, M. D., & Walker, R. N. F. 1994, A&A, 288, 581
Lane, A. P., Haas, M. R., et al. 1990, ApJ, 361, 132
Marston, A. P., Reach, W. T., Noriega-Crespo, A., et al. 2004, ApJS, 154, 333
Müller, H. S. P., Schlöder, F., et al. 2005, J. Mol. Struct, 742, 215
Mürtz, P., Zink, L. R., et al. 1998, J. Chem. Phys., 109, 9744
Ossenkopf, V., Röllig, M., Simon, R., et al. 2010, A&A, 518, L79
Pilbratt, G. L., Riedinger, J. R., Passvogel, T., et al. 2010, A&A, 518, L1
Polehampton, E. T., Baluteau, J., et al. 2007, MNRAS, 377, 1122
Röllig, M., Ossenkopf, V., et al. 2006, A&A, 451, 917
Sandell, G. 2000, A&A, 358, 242
Tapia, M., Persi, P., & Roth, M. 1996, ApJ, 340, 318
Hunter, T. R., Brogan, C. L, Megeath, S. T., et al. 2007, ApJ, 649, 888
Stäuber, P., & Bruderer, S. 2009, A&A, 505, 195
Strahan, S. E., Mueller, R. P., & Saykally, R. J. 1986, J. Chem. Phys., 85, 1252
van der Tak, F. F. S., Marseille, M. G., Herpin, F., et al. 2010, A&A, 518, L107
van Dishoeck, E., & Black, J. 1986, ApJS, 62, 109
Wehinger, P. A., Wyckoff, S., et al. 1974, ApJ, 190, L43
Weis, B., Carter, S., et al. 1989, J. Chem. Phys., 91, 2818
Zheng, R., Li, S., et al. 2008, Chin. Phys. B, 17, 4485

Page 5 is available in the electronic edition of the journal at http://www.aanda.org

[1] I. Physikalisches Institut der Universität zu Köln, Zülpicher Straße 77, 50937 Köln, Germany
e-mail: ossk@pk1.uni-koeln.de

[2] SRON Netherlands Institute for Space Research, P.O. Box 800, 9700 AV Groningen, The Netherlands

[3] California Institute of Technology, Pasadena, CA 91125 USA

[4] Max-Planck-Institut für Radioastronomie, Auf dem Hügel 69, 53121, Bonn, Germany

[5] University of Michigan, Ann Arbor, MI 48197 USA

[6] Laboratoire d'Astrophysique de Grenoble, UMR 5571-CNRS, Université Joseph Fourier, Grenoble, France

[7] Université de Bordeaux, Laboratoire d'Astrophysique de Bordeaux, France; CNRS/INSU, UMR 5804, Floirac, France

[8] Institute of Astronomy, ETH Zürich, 8093 Zürich, Switzerland

[9] Istituto Fisica Spazio Interplanetario INAF, via Fosso del Cavaliere 100, 00133 Roma, Italy

[10] Institut d'Astrophysique Spatiale, Université Paris-Sud, Bât. 121, 91405 Orsay Cedex, France

[11] LERMA & UMR 8112 du CNRS, Observatoire de Paris, 61, Av. de l'Observatoire, 75014 Paris, France

[12] School of Physics and Astronomy, University of Leeds, Leeds LS2 9JT UK

[13] Université de Toulouse, UPS, CESR, 9 avenue du colonel Roche, 31062 Toulouse Cedex 4, France

[14] CNRS, UMR 5187, 31028 Toulouse, France

[15] Centro de Astrobiología, CSIC-INTA, 28850, Madrid, Spain

[16] NAF Osservatorio Astrofisico di Arcetri, Florence Italy

[17] LERMA & UMR 8112 du CNRS, Observatoire de Paris and École Normale Supérieure, 24 rue Lhomond, 75231 Paris Cedex 05, France

[18] Astronomical Institute "Anton Pannekoek", University of Amsterdam, Amsterdam, The Netherlands

[19] Department of Astrophysics/IMAPP, Radboud University Nijmegen, Nijmegen, The Netherlands

[20] Université Pierre et Marie Curie, LPMAA UMR CNRS 7092, Case 76, 4 place Jussieu, 75252 Paris Cedex 05, France

[21] Observatorio Astronómico Nacional, Apdo. 112, 28803 Alcalá de Henares, Spain

[22] Jet Propulsion Laboratory, 4800 Oak Grove Drive, MC 302-231, Pasadena, CA 91109, USA

[23] Astronomy Department, University of Maryland, College Park, MD 20742, USA

[24] Ohio State University, Columbus, OH 43210, USA

[25] NRC/HIA Victoria, BC V9E 2E7, Canada

[26] Instituto de Radio Astronomía Milimétrica (IRAM), Avenida Divina Pastora 7, Local 20, 18012 Granada, Spain

[27] Department of Astronomy and Astrophysics, University of Toronto, 60 St. George Street, Toronto, ON M5S 3H8, Canada

[28] Department of Physics and Astronomy, University of Waterloo, Waterloo, ON N2L 3G1, Canada

[29] Institut für 4D-Technologien, FHNW, 5210 Windisch, Switzerland

[30] Center for Astrophysics, Cambridge MA 02138, USA

[31] Experimental Physics Dept., National University of Ireland Maynooth, Co. Kildare, Ireland

[32] Department of Physics and Astronomy, Johns Hopkins University, 3400 North Charles Street, Baltimore, MD 21218, USA

[33] INAF - Osservatorio Astronomico di Roma, Monte Porzio Catone, Italy

[34] Centre for Radio Astronomy, University of Calgary, Canada

[35] Kapteyn Astronomical Institute, University of Groningen, PO Box 800, 9700 AV Groningen, The Netherlands

[36] Leiden Observatory, Universiteit Leiden, PO Box 9513, 2300 RA Leiden, The Netherlands

[37] European Space Astronomy Centre, Urb. Villafranca del Castillo, PO Box 50727, Madrid 28080, Spain

[38] Department of Physics and Astronomy, University College London, London, UK

[39] Atacama Large Millimeter Array, Joint ALMA Office, Santiago, Chile

[40] Tata Institute of Fundamental Research (TIFR), Homi Bhabha Road, Mumbai 400005, India

[41] University of Western Ontario, Department of Physics & Astronomy, London, N6A 3K7 Ontario, Canada